ISSN: 3033-3326

Research Article

Journal of Chemotherapy and Cancer Research

Analysis and Control of Brain Dynamic Models

Lakshmi N Sridhar

Department Chemical Engineering, University of Puerto Rico, Mayaguez, Puerto Rico

***Corresponding author**
Lakshmi. N. Sridhar, Chemical Engineering Department University of Puerto Rico Mayaguez, Puerto Rico.

Received: May 12, 2025; **Accepted:** May 19, 2025; **Published:** May 28, 2025

ABSTRACT
The nonlinear behavior of the brain's information processing represents one of the key tasks in modern neuroscience, and a lot of research has been conducted in trying to rhythmicity in brain networks. Bifurcation analysis is a powerful mathematical tool used to deal with the nonlinear dynamics of any process. Several factors must be considered, and multiple objectives must be met simultaneously. Bifurcation analysis and multiobjective nonlinear model predictive control (MNLMPC) calculations are performed on two brain dynamic models. The MATLAB program MATCONT was used to perform the bifurcation analysis. The MNLMPC calculations were performed using the optimization language PYOMO in conjunction with the state-of-the-art global optimization solvers IPOPT and BARON. The bifurcation analysis Hopf bifurcation points that lead to limit cycles in the two models. These Hopf points were eliminated using an activation factor that involves the tanh function. The multiobjective nonlinear model predictive control calculations converge to the Utopia point in both the problems, which is the best solution.

Keywords: Bifurcation, Optimization, Control, Neuroscience, Brain, Hopf

Background

Yamaguchi showed that lecticans are organizers of the brain's extracellular matrix [1]. Manor et al. showed that synaptic depression mediates bistability in neuronal networks with recurrent inhibitory connectivity [2]. Oohashi et al demonstrated that Bral1, a brain-specific link protein, colocalizes with the versican v2 isoform at the nodes of Ranvier in developing and adult mouse central nervous systems [3]. Bekku et al performed the molecular cloning of bral2, a novel brain-specific link protein, and demonstrated the immunohistochemical colocalization with brevican in perineuronal nets [4]. Dityatev et al showed the synaptic plasticity of extracellular matrix molecules [5]. Carulli et al. determined the composition of perineuronal nets in the adult rat cerebellum and the cellular origin of their components [6].

Rich and Wenner researched sensing and expressing homeostatic synaptic plasticity [7]. Dityatev et al investigated the activity-dependent formation and functions of chondroitin sulfate-rich extracellular matrix of perineuronal nets [8]. Turrigiano showed that homeostatic signaling was the positive side of negative feedback [9]. Xie et al demonstrated the existence of Hopf bifurcations in the Hodgkin-Huxley model [10]. Cingolani et al. investigated the activity-dependent regulation of synaptic AMPA receptor composition and abundance by beta 3 integrins [11].

Durstewitz discussed the implications of synaptic biophysics for recurrent network dynamics and active memory [12]. Dityatev remodeled the extracellular matrix and epileptogenesis [13]. Kochlamazashvili et al. showed that the extracellular matrix molecule hyaluronic acid regulates hippocampal synaptic plasticity by modulating postsynaptic l-type ca(2+) channels [14]. Dityatev et al. demonstrated that the extracellular matrix played a dual role in synaptic plasticity and homeostasis [15]. Dityatev and Rusakov demonstrated the existence of molecular signals of plasticity at the tetrapartite synapse [16]. Wlodarczyk et al. showed the role played by extracellular matrix molecules, their receptors, and secreted proteases in synaptic plasticity [17]. Kazantsev et al. developed a homeostatic model of neuronal firing governed by feedback signals from the extracellular matrix [18].

Soleman et al. investigated the targeting of the neural extracellular matrix in neurological disorders [19]. Dembitskaya et al studied the effects of enzymatic removal of chondroitin sulfates on neural excitability and synaptic plasticity in the hippocampal CA1 region [20]. Favuzzi et al. investigated the

Citation: Lakshmi N Sridhar. Analysis and Control of Brain Dynamic Models. J Chem Can Res. 2025. 3(2): 1-6. DOI: doi.org/10.61440/JCCR.2025.v3.22

activity-dependent gating of parvalbumin interneuron function by the perineuronal net protein brevican [21]. Jercog et al demonstrated that the cortical dynamics reflect state transitions in a bistable network [22]. Schmidt et al showed that the network mechanisms cause oscillations in cognitive tasks [23]. Azeez et al. demonstrated the diurnal fluctuation of extracellular matrix organization in the lateral hypothalamus in basal conditions and in neuroinflammation [24].

Song and Dityatev investigated the interaction between glia, extracellular matrix and neurons [25]. Lazarevichet al demonstrated the existence of activity-dependent switches between dynamic regimes of extracellular matrix expression [26]. Rozhnova et al showed the impact of the brain extracellular matrix on neuronal firing reliability and spike-timing jitter [27]. Rozhnova demonstrated the chaotic change of extracellular matrix molecules concentration in the presence of periodically varying neuronal firing rate [28]. Rozhnova et al. performed bifurcation analysis calculations on a model of brain extracellular matrix [29].

This work aims to perform bifurcation and multiobjective nonlinear model predictive control(MNLMPC) on two brain dynamics models, which are Brain extracellular matrix model of Rozhnova et al. and the Hodgkin-Huxley model of Xie et al [10,29]. This document is organized as follows. The model equations for both the models are first described. This is followed by a description of the numerical methods (bifurcation analysis and MNLMPC). The results and discussion are then presented, followed by the conclusions.

Brain Dynamics models

Model 1 : Brain extracellular matrix model [29].

The equations in this model are

$$\frac{dzval}{dt} = -(\alpha_z + \gamma_p)zval + \beta_z F_z$$
$$\frac{dpval}{dt} = -\alpha_p pval + \beta_p F_p$$
$$F_z = z_0 - \frac{z_0 - z_1}{1 + \exp(\frac{-Q-\theta_z}{k_z})} \quad (1)$$
$$F_p = z_0 - \frac{p_0 - p_1}{1 + \exp(\frac{-Q-\theta_p}{k_p})}$$
$$Q = Q_0 + \alpha_Q zval$$

The parameter values are

$Q_0 = 5; \alpha_Q = 0.23; \alpha_Z = 0.001; \alpha_p = 0.001; \gamma_P = 0.001; \beta_Z = 0.01;$
$z_0 = 0; z_1 = 1; p_0 = 0; p_1 = 1; k_z = 0.15; k_p = 0.05; \beta_p = 0.01$

zval and pval represent the concentration of the ECM molecules and the concentration of proteases. θ_z, θ_p are the activation midpoints and are the bifurcation and control parameters.

Model 2: Hodgkin-Huxley model [10].

The equations in this model are

$$\frac{d(vval)}{dt} = \frac{1}{C_M}(I_{EXT} - g_{Na}(mval)^3 hval(vval - vna) - g_K(nval)^4(vval - v_K) - g_L(vval - v_L))$$
$$\frac{d(mval)}{dt} = \alpha_m(1 - mval) - \beta_m(mval)$$
$$\frac{d(hval)}{dt} = \alpha_h(1 - hval) - \beta_h(hval) \quad (2)$$
$$\frac{d(nval)}{dt} = \alpha_n(1 - hval) - \beta_n(hval)$$

Where $\alpha_m, \beta_m, \alpha_h, \beta_h, \alpha_n, \beta_n$ are defined as

$$\alpha_m = 0.1\frac{(25 - vval)}{\{\exp(\frac{25 - vval}{10}) - 1\}}$$
$$\beta_m = 4\exp(-\frac{vval}{18})$$
$$\alpha_h = 0.07\exp(-\frac{vval}{20}) \quad (3)$$
$$\beta_h = \frac{1}{\{\exp(\frac{30 - vval}{10}) + 1\}}$$
$$\alpha_n = \frac{0.01(10 - vval)}{\{\exp(\frac{10 - vval}{10}) - 1\}}$$
$$\beta_n = 0.125\exp(-\frac{vval}{80})$$

The parameters are

$V_{Na} = 115.0$, $V_K = -12.0$, $V_L = 10.599, g_{Na} = 120.0, g_K = 36$, $g_L = 0.3, C_M = 1$

vval is the electrical potential difference voltage across the nerve membrane (membrane potential). *mval* and *hval* represent the gating variables for the activation and inactivation of the sodium ion channel, respectively. nval is the activation gating variable of the potassium ion channel. I_{EXT} is the external current and the bifurcation and control parameter.

Numerical Procedures

Bifurcation analysis

The MATLAB software MATCONT is used to perform the bifurcation calculations. Bifurcation analysis deals with multiple steady-states and limit cycles. Multiple steady states occur because of the existence of branch and limit points. Hopf bifurcation points cause limit cycles. A commonly used MATLAB program that locates limit points, branch points, and Hopf bifurcation points is MATCONT [30,31]. This program detects Limit points (LP), branch points (BP), and Hopf bifurcation points(H) for an ODE system

$$\frac{dx}{dt} = f(x, \alpha) \quad (4)$$

$x \in R^n$ Let the bifurcation parameter be α Since the gradient is orthogonal to the tangent vector,

T he tangent plane at any point $w = [w_1, w_2, w_3, w_4, \ldots w_{n+1}]$ must satisfy

$$Aw = 0 \quad (5)$$

Where A is

$$A = [\partial f / \partial x \quad | \partial f / \partial \alpha] \quad (6)$$

where $\partial f / \partial x$ is the Jacobian matrix. For both limit and branch points, the matrix $[\partial f / \partial x]$ must be singular. The n+1 th component of the tangent vector $w_{n+1} = 0$ for a limit point (LP)and for a branch point (BP) the matrix $\begin{bmatrix} A \\ w^T \end{bmatrix}$ must be singular. At a Hopf bifurcation point,

$$\det(2f_x(x,a)@I_n) = 0 \quad (7)$$

@ indicates the bialternate product while I_n is the n-square identity matrix. Hopf bifurcations cause limit cycles and should be eliminated because limit cycles make optimization and control

tasks very difficult. More details can be found in Kuznetsov and Govaerts [32-34].

Hopf bifurcations cause unwanted oscillatory behavior and limit cycles. The tanh activation function (where a control value u is replaced by) (u tanh u/ε) is commonly used in neural nets and optimal control problems to eliminate spikes in the optimal control profile [35-38]. Hopf bifurcation points cause oscillatory behavior. Oscillations are similar to spikes, and the results in Sridhar demonstrate that the tanh factor also eliminates the Hopf bifurcation by preventing the occurrence of oscillations [39]. Sridhar explained with several examples how the activation factor involving the tanh function successfully eliminates the limit cycle causing Hopf bifurcation points [39]. This was because the tanh function increases the time period of the oscillatory behavior, which occurs in the form of a limit cycle caused by Hopf bifurcations.

Multiobjective Nonlinear Model Predictive Control (MNLMPC)

Flores Tlacuahuaz et al developed a multiobjective nonlinear model predictive control (MNLMPC) method that is rigorous and does not involve weighting functions or additional constraints [30]. This procedure is used for performing the MNLMPC calculations Here $\sum_{t_i=0}^{t_i=t_f} q_j(t_i)$ (j=12..n) represents the variables that need to be minimized/maximized simultaneously for a problem involving a set of ODE.

$$\frac{dx}{dt} = F(x,u) \tag{7}$$

t_f being the final time value, and n the total number of objective variables and the control parameter. This MNLMPC procedure first solves the single objective optimal control problem independently optimizing each of the variables $\sum_{t_i=0}^{t_i=t_f} q_j(t_i)$ individually. The minimization/maximization of $\sum_{t_i=0}^{t_i=t_f} q_j(t_i)$ will lead to the values q_j^* Then the optimization problem that will be solved is

$$\min\left(\sum_{j=1}^{n}\left(\sum_{t_i=0}^{t_i=t_f} q_j(t_i) - q_j^*\right)\right)^2 \tag{8}$$
$$subject\ to\ \frac{dx}{dt} = F(x,u);$$

This will provide the values of u at various times. The first obtained control value of u is implemented and the rest are discarded. This procedure is repeated until the implemented and the first obtained control values are the same or if the Utopia point where $\left(\sum_{t_i=0}^{t_i=t_f} q_j(t_i) = q_j^*\ for\ all\ j\right)$ is obtained.

Pyomo is used for these calculations [31]. Here, the differential equations are converted to a Nonlinear Program (NLP) using the orthogonal collocation method The NLP is solved using IPOPT and confirmed as a global solution with BARON [32,33].

The steps of the algorithm are as follows

1. Optimize $\sum_{t_i=0}^{t_i=t_f} q_j(t_i)$ and obtain q_j^* at various time intervals t_i. The subscript i is the index for each time step.
2. Minimize $\left(\sum_{j=1}^{n}\left(\sum_{t_i=0}^{t_i=t_f} q_j(t_i) - q_j^*\right)\right)^2$ and get the control values for various times.
3. Implement the first obtained control values
4. Repeat steps 1 to 3 until there is an insignificant difference between the implemented and the first obtained value of the control variables or if the Utopia point is achieved. The Utopia point is when $\sum_{t_i=0}^{t_i=t_f} q_j(t_i) = q_j^*$ for all j.

Results and Discussion

For the bifurcation analysis in model 1, both θ_p and θ_z were individually used as bifurcation parameters. When θ_p was used as a bifurcation parameter, two Hopf bifurcation points were found at $(zval, pval, \theta_p)$ values of (2.128943 0.426793 5.645178) and (4.230053 1.696697 6.052311). These Hopf bifurcation points are shown in Figure. 1a. Each of these Hopf bifurcation points result in a limit cycle which are shown in figures 1b and 1c. When θ_p was modified to $\frac{\theta_p \tanh(\theta_p)}{1.115}$ the hopf bifurcations disappear (Figure. 1d).

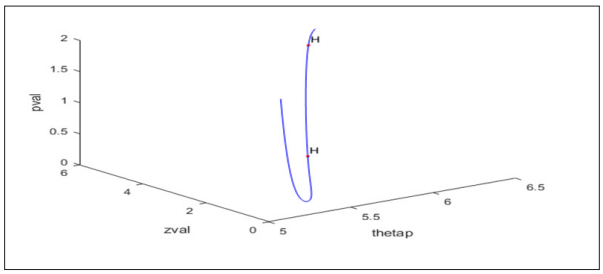

Figure 1a

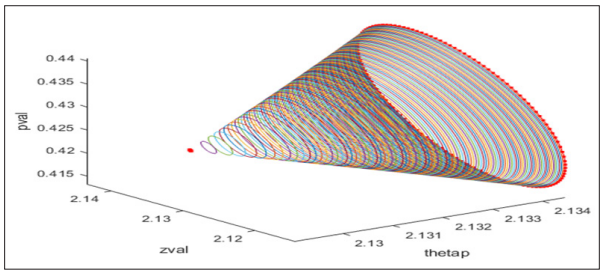

Figure 1b

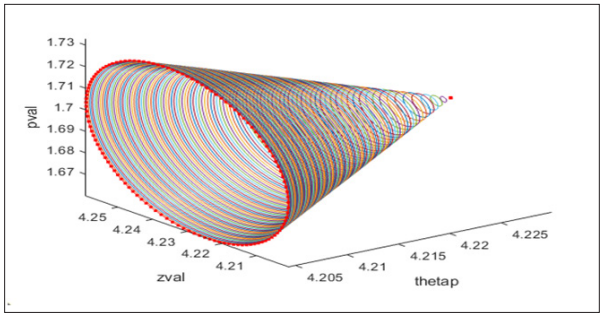

Figure 1c

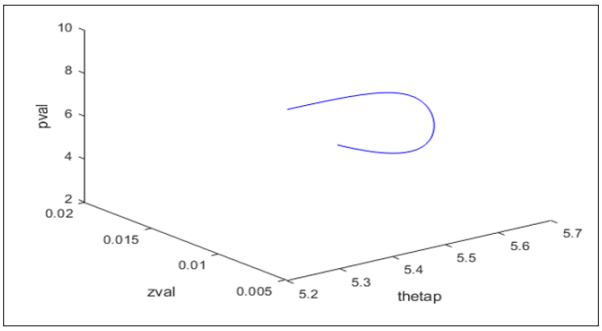

Figure 1d

When θ_z was used as a bifurcation parameter, two Hopf bifurcation points were found at (*zval, pval,* θ_z) values of (2.696435 0.266904 5.951550) and (3.190589 2.102711 5.604739) These Hopf bifurcation points are shown in Figure. 1e. Each of these Hopf bifurcation points result in a limit cycle which are shown in figures 1f and 1g. When θ_z was modified to $\frac{\theta_z \tanh(\theta_z)}{1.115}$ the hopf bifurcations disappear (Figure. 1h).

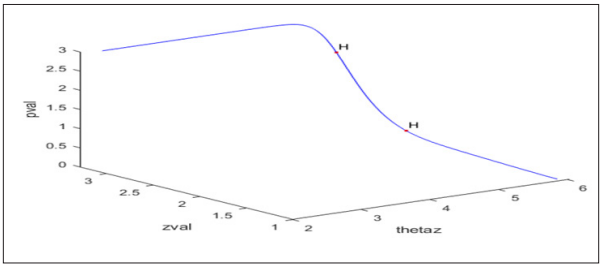

Figure 1e

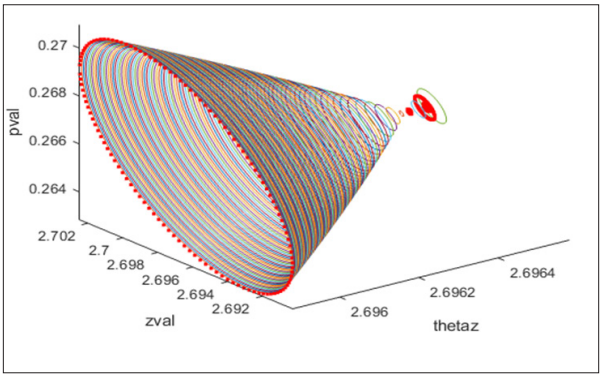

Figure 1f

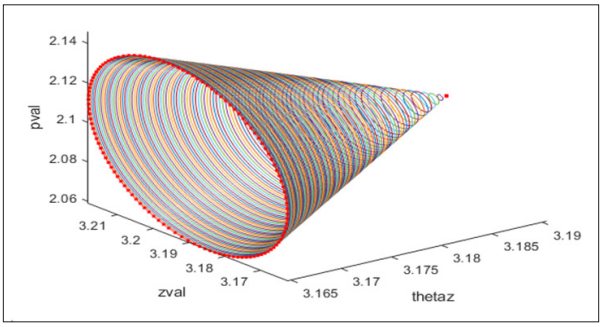

Figure 1g

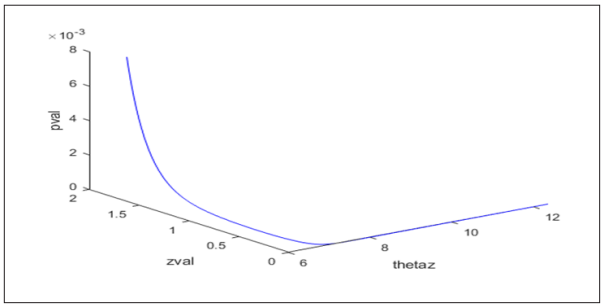

Figure 1h

The MNLMPC calculations were performed using $\frac{\theta_p \tanh(\theta_p)}{1.115}$ and $\frac{\theta_z \tanh(\theta_z)}{1.115}$ as the control parameters. $\sum_{t_i=0}^{t_i=t_f} zval_j(t_i)$ (ECM concentration) was maximized and resulted in a value of 20. $\sum_{t_i=0}^{t_i=t_f} pval_j(t_i)$ (proteas concentration) was minimized and resulted in a value of 0. The multiobjective optimal control calculation involved a minimization of $\left(\sum_{t_i=0}^{t_i=t_f} zval_j(t_i)-20\right)^2+\left(\sum_{t_i=0}^{t_i=t_f} pval_j(t_i)-0\right)^2$. This minimization resulted in the Utopia point (0). The first of the control variables is implemented, and the rest are discarded. The process is repeated until the difference between the first and second values of the control variables are the same. The MNLMPC control values of both θ_p and θ_z were 5 and 5. The zval and pval profiles are shown in Figures 1i and 1j.

In model 2, I_{EXT} is the bifurcation parameter and a Hopf bifurcation point was found at (vval, mval, hval, nval, 2, I_{EXT}) values of (5.345857 0.097257 0.406228 0.401784 9.779639). This is shown in Figure. 2a. The limit cycle produced by this Hopf bifurcation is shown in Figure. 2b. When I_{EXT} is modified to $\frac{I_{EXT} \tanh(I_{EXT})}{1.5}$ the Hopf Bifurcation point disappears.

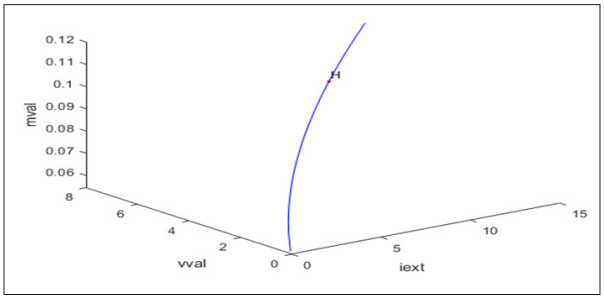

Figure 2a

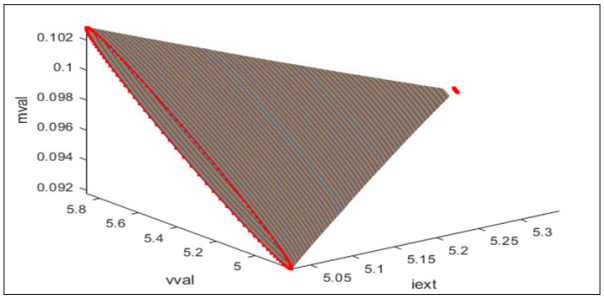

Figure 2b

For the MNLMPC calculations, $\sum_{t_i=0}^{t_i=t_f} vval_j(t_i), \sum_{t_i=0}^{t_i=t_f} mval_j(t_i), \sum_{t_i=0}^{t_i=t_f} nval_j(t_i)$ were maximized and resulted in values of 20,20 and 17.3647. $\sum_{t_i=0}^{t_i=t_f} hval_j(t_i)$, was minimized and resulted in a value of 0.

The multiobjective optimal control calculation involved a minimization of

$(\sum_{t_i=0}^{t_i=t_f} vval_j(t_i)-20)^2+(\sum_{t_i=0}^{t_i=t_f} mval_j(t_i)-20)^2+(\sum_{t_i=0}^{t_i=t_f} nval_j(t_i)-17.3647)^2+(\sum_{t_i=0}^{t_i=t_f} hval_j(t_i)-0)^2$.

$\frac{I_{EXT}\tanh(I_{EXT})}{1.5}$ was used as the control parameter.

This minimization resulted in the Utopia point (0). The first of the control variables is implemented, and the rest are discarded. The process is repeated until the difference between the first and second values of the control variables are the same. The MNLMPC control value of I_{EXT} is 1. The vval, hval and nval profiles for the MNLMPC calculations are shown in figures 2d and 2e. The mval value was 1 throughout.

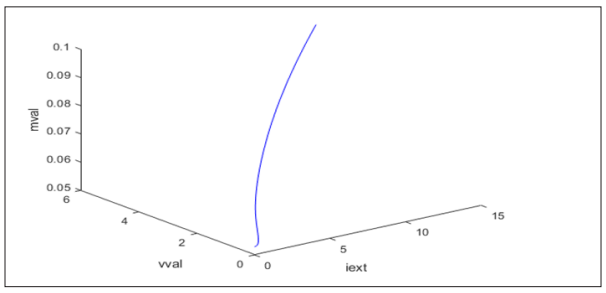

Figure 2c

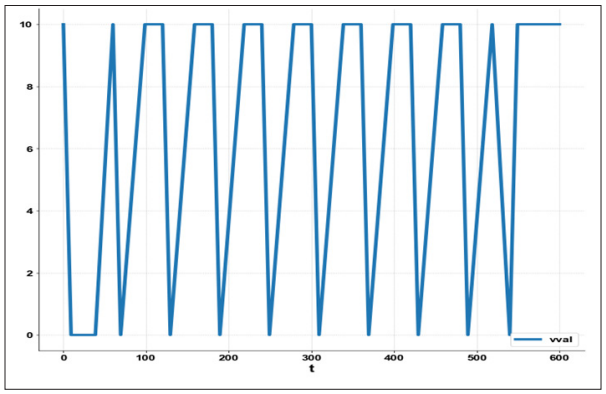

Figure 2d

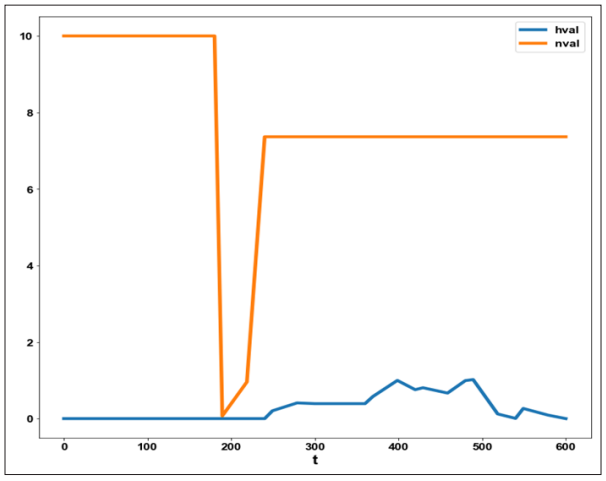

Figure 2e

Both brain models show the presence of limit cycles causing Hopf bifurcations, which can be eliminated using the activation factor involving the tanh function, confirming the analysis of Sridhar(2024). In both cases, the MNLMPC calculations converge to the Utopia solution.

Conclusions

Multiobjective nonlinear model predictive control calculations were performed along with bifurcation analysis on two models involving brain dynamics. The bifurcation analysis revealed the existence of limit cycle causing Hopf bifurcation points, which are eliminated using an activation factor involving the tanh function. The multiojective nonlinear model predictive calculations converge to the Utopia point(the best possible solution) .in both models.

Data Availability Statement

All data used is presented in the paper

Conflict of interest

The author, Dr. Lakshmi N Sridhar has no conflict of interest.

Acknowledgement

Dr. Sridhar thanks Dr. Carlos Ramirez and Dr. Suleiman for encouraging him to write single-author papers.

References

1. Yamaguchi Y. Lecticans: organizers of the brain extracellular matrix. Cellular and Molecular Life Sciences. CMLS. 2000. 57: 276-89.
2. Manor Y, Nadim F. Synaptic depression mediates bistability in neuronal net- works with recurrent inhibitory connectivity. J Neurosci 2001. 2: 9460–9470.
3. Oohashi T, Hirakawa S, Bekku Y, Rauch U, Zimmermann DR, et al. A brain-specific link protein, colocal- izing with the versican v2 isoform at the nodes of ranvier in developing and adult mouse central nervous systems. Mol. Cell. Neurosci. 2002. 19: 43-57.
4. Bekku Y, Su W-D, Hirakawa S, Fässler R, Ohtsuka A, et al. Molecular cloning of bral2, a novel brain-specific link protein, and immunohistochemical colocalization with bre- vican in perineuronal nets. Mol Cell Neurosci. 2003. 24:148-59.
5. Dityatev A, Schachner M. Extracellular matrix molecules and synaptic plastic- ity. Nat Rev Neurosci. 2003. 4: 456-468.
6. Carulli D, Rhodes KE, Brown DJ, Bonnert TP, Pollack SJ, et al. Compo- sition of perineuronal nets in the adult rat cerebellum and the cellular origin of their components. J Comp Neurol. 2006. 494: 55-577.
7. Rich MM, Wenner P. Sensing and expressing homeostatic synaptic plasticity. Trends Neurosci. 2007. 30: 119-125.
8. Dityatev A, Brückner G, Dityateva G, Grosche J, Kleene R, et al. Activi-ty-dependent formation and functions of chondroitin sulfate-rich extracellular matrix of perineuronal nets. Dev Neurobiol. 2007. 67: 570-588.
9. Turrigiano G. Homeostatic signaling: the positive side of negative feedback. Curr Opin Neurobiol. 2007. 17: 318-324.
10. Xie Yong, Chen Luonan, Kang Yan Mei, Aihara Kazuyuki. Controlling the onset of Hopf bifurcation in the Hodgkin-Huxley model. Phys Rev E. 2008. 77.
11. Cingolani LA, Lorenzo A, Thalhammer A, Lily MY, Yu LMY, et al. Activity-dependent regulation of synaptic AMPA receptor composition and abundance by beta 3 integrins. Neuron. 2008. 58: 749-762.

12. Durstewitz D. Implications of synaptic biophysics for recurrent network dynamics and active memory. Neural Networks. 2009. 22: 1189-1200.
13. Dityatev A. Remodeling of extracellular matrix and epileptogenesis. Epilepsia. 2010. 51: 61-65.
14. Kochlamazashvili G, Henneberger C, Bukalo O, Dvoretskova E, Senkov O, et al. The extracellular matrix molecule hyaluronic acid regulates hip- pocampal synaptic plasticity by modulating postsynaptic l-type ca(2+) chan- nels. Neuron. 2010. 67: 116-128.
15. Dityatev A, Schachner M, Sonderegger P. The dual role of the extra- cellular matrix in synaptic plasticity and homeostasis. Nat Rev Neurosci. 2010. 11: 735-746.
16. Dityatev A, Rusakov D. Molecular signals of plasticity at the tetrapartite synapse. Curr Opin Neurobiol. 2011. 21: 353-359.
17. Wlodarczyk J, Mukhina I, Kaczmarek L, Dityatev A. Extracellular matrix molecules, their receptors, and secreted proteases in synaptic plasticity. Dev Neurobiol. 2011. 71: 1040-1053.
18. Kazantsev V, Gordleeva S, Stasenko S, Dityatev A. A homeostatic model of neuronal firing governed by feedback signals from the extracellular matrix. PLoS ONE. 2012. 7: e41646 .
19. Soleman S, Filippov MA, Dityatev A, Fawcett JW. Targeting the neural extracellular matrix in neurological disorders. Neuroscience. 2013. 253: 194-213.
20. Dembitskaya Y, Song I, Doronin M, Dityatev A, Semyanov A. Effects of enzy- matic removal of chondroitin sulfates on neural excitability and synaptic plas- ticity in the hippocampal CA1 region. 9th FENS Meeting. Milan. Italy. 2014. 5-9.
21. Favuzzi E, Marques-Smith A, Deogracias R, Winterflood CM, Sánchez-Aguil- era A, et al. Activity-dependent gating of parvalbumin interneuron function by the perineuronal net protein brevican. Neuron. 2017. 95: 639-655.
22. Jercog D, Roxin A, BarthóP, Luczak A, Compte A, et al. UP-DOWN Cortical dynamics reflect state transitions in a bistable network. Elife. 2017. 6: e22425.
23. Schmidt H, Avitabile D, MontbrióE, Roxin A. Network mechanisms un- derlying the role of oscillations in cognitive tasks. PLoS Comput Biol. 2018. 14: e1006430.
24. Azeez IA, Tesoriero C, Scambi I, Mariotti R, Bentivoglio M. Diurnal fluctuation of extracellular matrix organization in the lateral hypothalamus in basal con- ditions and in neuroinflammation. 11th FENS Forum of Neuroscience. Berlin. 2018. 7-11.
25. Song I, Dityatev A. Crosstalk between glia, extracellular matrix and neurons. Brain Res Bull. 2018. 136: 101-108.
26. Lazarevich I, Stasenko S, Rozhnova M, Pankratova E, Dityatev A, et al. Activity-dependent switches between dynamic regimes of extracellular matrix expression. PLoS ONE. 2020. 15: e0227917 .
27. Rozhnova MA, Pankratova EV, Kazantsev VB. Brain extracellular matrix impact on neuronal firing reliability and spike-timing jitter. In: Advances in Neural Computation, Machine Learning, and Cognitive Research III (Part of the Studies in Computational Intelligence book series. 2020. 856: 190-196.
28. Rozhnova MA, Bandenkov DV, Kazantsev VB, Pankratova EV. Chaotic change of extracellular matrix molecules concentration in the presence of periodically varying neuronal firing rate. Communications in Computer and In- formation Science, Mathematical Modeling and Supercomputer Technologies. 2021. 1413: 117-128.
29. Rozhnova MA, Evgeniya V, Pankratova Sergey V, Stasenko Victor B, Kazantsev. Bifurcation analysis of multistability and oscillation emergence in a model of brain extracellular matrix. Chaos. Solitons & Fractals. 2021. 151: 111253.
30. Dhooge A, Govearts W, Kuznetsov AY. MATCONT. A Matlab package for numerical bifurcation analysis of ODEs. ACM transactions on Mathematical software. 2003. 29: 141-164.
31. Dhooge A, Govaerts W, Kuznetsov YA, Mestrom W, Riet AM. CL_MATCONT. A continuation toolbox in Matlab. 2004.
32. Kuznetsov YA. Elements of applied bifurcation theory. Springer. NY. 1998.
33. Kuznetsov YA. Five lectures on numerical bifurcation analysis. Utrecht University. NL. 2009.
34. Govaerts wJF. Numerical Methods for Bifurcations of Dynamical Equilibria. SIAM. 2000.
35. Dubey SR, Singh SK, Chaudhuri BB. Activation functions in deep learning: A comprehensive survey and benchmark. Neurocomputing. 2022. 503: 92-108.
36. Kamalov AF, Nazir M, Safaraliev AK, Cherukuri, Zgheib R. Comparative analysis of activation functions in neural networks. 28th IEEE International Conference on Electronics, Circuits, and Systems (ICECS). Dubai. United Arab Emirates. 2021. 1-6.
37. Szandała T. Review and Comparison of Commonly Used Activation Functions for Deep Neural Networks. ArXiv. 2020.
38. Sridhar LN. Bifurcation Analysis and Optimal Control of the Tu¬mor Macrophage Interactions. Biomed J Sci & Tech Res. 2023. 53.
39. Sridhar LN. Elimination of oscillation causing Hopf bifurcations in engineering problems. Journal of Applied Math. 2024b. 2: 1826.
40. Flores-Tlacuahuac A. Pilar Morales and Martin Riveral Toledo. Multiobjective Nonlinear model predictive control of a class of chemical reactors . I & EC research. 2012. 5891-5899.
41. Hart William E, Carl D Laird, Jean-Paul Watson, David L Woodruff, Gabriel A Hackebeil, et al. Pyomo – Optimization Modeling in Python. Second Edition. 2017. 67.
42. Wächter A, Biegler L. On the implementation of an interior-point filter line-search algorithm for large-scale nonlinear programming. Mat. Program. 2006. 106: 25-57.
43. Tawarmalani M, Sahinidis NV. A polyhedral branch-and-cut approach to global optimization. Mathematical Programming. 2005. 103: 225-249.